in Table I represent "true" widths within the limitations inherent in the model. The over-all correctness of these error assignments has been checked in two ways. First, the experimental distribution of χ^2 for the kinematic fit of the events in the data sample is found to have a mean value of 0.83, where 1.0 is expected. Secondly, since the missing mass squared to the proton and its error are the quantities of interest, it is desirable to examine a system in which this missing mass is a δ function, and to compare the calculated resolution width with the width of the experimentally observed distribution. This has been done using a sample of elastic scattering events from the same film. The elastic events (identified by a four-constraint fit) were refitted using one constraint only, ignoring the outgoing π^+ momentum vector. The resolution width computed from the most probable error for these events is 0.047 GeV^2, while the width of the observed distribution of missing mass squared is found to be 0.042 GeV^2.

*Work done under the auspices of the U. S. Atomic Energy Commission.

[1]W. Michael and G. Gidal, Phys. Rev. Letters 28, 1475 (1972).
[2]J. MacNaughton, W. R. Butler, D. G.Coyne, C. Fu, and G. H. Trilling, LBL Report No. UCRL-20833 (unpublished).
[3]J. P. Baton *et al.*, Phys. Letters 33B, 528 (1970).
[4]P. E. Schlein, Lecture Notes for the International School of Subnuclear Physics, Erice, Sicily, 1970 (unpublished).
[5]K. Boesebeck *et al.*, Nucl. Phys. B28, 381 (1971).
[6]The maximization was done with the program OPTIME by Philippe Eberhard and Werner O. Koellner, LBL Reports No. UCRL-20159, No. UCRL-20160 (unpublished).
[7]J. D. Jackson, Nuovo Cimento 34, 1644 (1964).
[8]D. G. Coyne *et al.*, Nucl. Phys. B32, 333 (1971).

PHYSICAL REVIEW D VOLUME 7, NUMBER 7 1 APRIL 1973

Experimental Comparison of *CP* Violation in $\overline{K}^0 \to \pi^+\pi^-$ and $K^0 \to \pi^+\pi^-$ Decays*

D. Banner,† J. Frank,‡ M. Gormley, L. J. Koester, S. Raither,§ J. H. Smith, and A. Wattenberg
University of Illinois at Urbana-Champaign, Urbana, Illinois 61801

(Received 21 August 1972)

The time distributions of the decays $K^0 \to \pi^+\pi^-$ and $\overline{K}^0 \to \pi^+\pi^-$ are directly compared in the same apparatus. K^0 ($\overline{K}^0$) mesons were produced by charge exchange of K^+ (K^-) in a carbon target. Wire spark chambers with magnetostrictive readout were used to detect the decays. The observation of the difference in the decay distributions of K^0 and $\overline{K}^0$ mesons serves as a direct proof, independent of any theoretical conventions, that *CP* is violated. No significant deviation from the presently accepted theoretical formalism of *CP* violation was found. The values of the *CP*-violating parameters for K^0 and $\overline{K}^0$ decays are compared.

I. INTRODUCTION

In 1964, the observation of the decay $K_L^0 \to \pi^+\pi^-$ by Christenson *et al.*[1] was immediately considered as evidence for *CP* violation. A variety of early alternative explanations were eliminated by experiments. Sakurai and Wattenberg[2] pointed out that vacuum-regeneration experiments such as that first performed with K^0 mesons by Böhm *et al.*[3] when combined with a similar $\overline{K}^0$ measurement, could establish that *CP* is really violated without recourse to any theoretical convention. In an experiment without an electric or magnetic field, if one observes a difference in the decay distribution from $\overline{K}^0$ and K^0 mesons, then one can experimentally distinguish between a particle and an antiparticle world. This could be considered an "experimental" definition of *CP* violation.

In the original paper discussing the K^0-$\overline{K}^0$ system, Lee, Oehme, and Yang[4] state or imply that many assumptions are involved in the theoretical formalism for *CP* violation. The assumptions include: the *CPT* theorem, the superposition principle, the Wigner-Weisskopf hypothesis, the Hermitian nature of the fields, the existence of only two neutral *K* mesons, etc. Regeneration experiments have been analyzed by Darriulat *et al.*[5] as evidence against particle mixtures and in support of the *CP*-

violation interpretation. However, there have continued to be theoretical papers published questioning whether there is experimental evidence for most of the other above assumptions, as for example, the papers by Kabir[6] and Llalović.[7] These latter authors also point out that a crucial measurement is a comparison of the K^0 and $\overline{K}^0$ interference in vacuum regeneration.

With the above assumptions of Lee, Oehme, and Yang, the expected behavior for K^0 and $\overline{K}^0$ decays as a function of time is

$$\left\{\begin{matrix} K^0 \\ \overline{K}^0 \end{matrix}\right\} \to \pi^+\pi^- \propto e^{-\gamma_S t} + |\eta|^2 e^{-\gamma_L t} \pm 2|\eta| e^{-(\gamma_S+\gamma_L)t/2} \cos(\Delta m t - \phi) . \quad (1)$$

Direct experimental evidence on $\overline{K}^0$ decays does not exist because all previous experiments have started with predominantly K^0 beams (70% by Böhm *et al.*[3] to 97% by Jensen *et al.*[8]) produced by protons (or pions) on complex nuclei. There is some indirect information on the $\overline{K}^0$ decays from such experiments, but in general the fraction of $\overline{K}^0$ mesons present had an uncertainty commensurate with the fraction present.[9]

This paper reports an experiment that directly demonstrates the reversal of the sign of the interference term in Eq. (1).

II. EXPERIMENTAL DETAILS

A beam of 850-MeV/c K^+ (K^-) mesons was used to produce K^0 ($\overline{K}^0$) mesons by means of charge exchange in a carbon target. Their subsequent decay into $\pi^+\pi^-$ pairs was observed in an array of magnetostrictive wire spark chambers and scintillation counters. Extrapolation of the pion tracks to their point of intersection determined the decay point. The trajectory of the incoming charged kaon was determined with a set of small wire spark chambers in the beam. The carbon target was thick, so the location along the trajectory at which the charge exchange occurred was found by dividing the target into wafers separated by scintillation counters. The production point and decay point determined the neutral-kaon direction, and knowledge of the angles made by the decay pions with respect to this direction allowed an unambiguous determination of the neutral-kaon momentum and consequently its proper decay time. The distribution of these decay times constituted the data of this experiment.

A. The Beam

The experiment was performed in a partially separated 850-MeV/c $K^\pm$ beam of the Zero-Gradient Synchrotron (ZGS) at the Argonne National Laboratory. A description of the beam transport system can be found elsewhere.[10] The system employed a 10-ft-long electrostatic separator with crossed electric and magnetic fields. The measured π/K ratio at the final focus was 13:1 for the negative beam and 4:1 for the positive beam, for a typical separator field of 140 kV/in. Approximately 5000 K^- and 25 000 K^+ mesons were transmitted to the final focus per typical ZGS pulse of 500-msec duration. The momentum

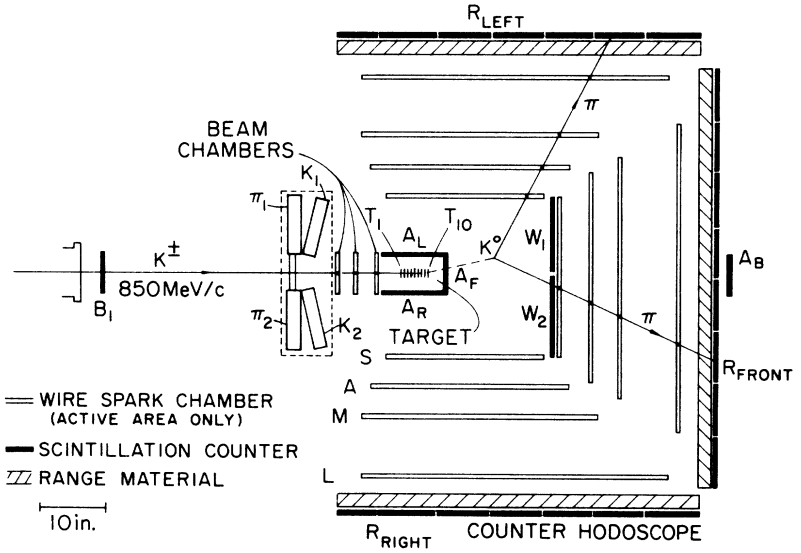

FIG. 1. Plan view of the experimental arrangement. Scintillators T_1–T_{10} are the target counters. Phototubes π_1, π_2 and K_1, K_2 receive Cherenkov light from beam pions and kaons, respectively.

spread of the beam was about ±4%, the divergence ±4 deg horizontally and ±0.6 deg vertically, and the final spot size 1.25 in.×1.25 in.

The large pion contamination in the beam was reduced to 5.0% for the negative beam and 1.2% for the positive beam by using a Cherenkov counter in the beam trigger. This Cherenkov counter was located between beam counters B_1 and T_1 (Fig. 1). Its radiator consisted of an ultraviolet transmitting Lucite slab, $\frac{3}{4}$ in. thick×2 in. high ×5 in. wide. Cherenkov light from pions was internally reflected into the pion phototubes (C_π), while light radiated by kaons escaped the Lucite slab and was reflected by means of a system of mirrors into the two kaon phototubes (C_K). The trigger logic for an incoming $K^\pm$ meson was $B_1 T_1 C_K \bar{C}_\pi$.

B. Determination of the Production Point

The trajectory of the incoming $K^\pm$ was measured in a set of three aluminum wire spark chambers with magnetostrictive readout. Each of the chambers consisted of two orthogonal wire planes separated by a gap of $\frac{3}{8}$ in. The middle chamber was rotated by 45 deg with respect to the other two chambers and was used to resolve pairing ambiguities which arise in the presence of more than one track. The material of each chamber corresponded to 1.7×10^{-3} radiation length.

In order to determine the position of the production point along the trajectory, the high-density graphite target (density = 2.2 g/cm^3) was divided into nine wafers, each $\frac{5}{16}$ in. thick×2 in. wide×1.75 in. high. These were sandwiched between ten scintillation counters, T_1 to T_{10}, each $\frac{1}{16}$ in. thick (Fig. 2). The anode signal was subjected to a crude two-level pulse-height analysis, the result of which was recorded by two gated latches. The minimum-ionizing $K^\pm$-beam particles triggered the low-threshold latch, whereas protons with momenta smaller than 550 MeV/c set both low- and high-threshold latches.

A K^- meson undergoes charge exchange and produces a $\bar{K}^0$ meson in the reaction

$$K^- + p \rightarrow n + \bar{K}^0 .$$

Thus a K^- charge exchange sets all of the low-threshold latches upstream of the interaction as in the following example.

Example 1 – a neutral ending:

Low-threshold latches	1 1 1 1 1 1 0 0 0 0,
High-threshold latches	0 0 0 0 0 0 0 0 0 0.

No high-threshold latch is set because any cascade or evaporation prongs are presumably of too low an energy to escape from the wafer in which the reaction occurs. 70% of all detected K^- charge exchanges are of this kind called a "neutral ending".

A K^+ meson undergoes charge exchange by the reaction

$$K^+ + n \rightarrow p + K^0$$

and therefore produces a relatively fast proton. This proton may, nevertheless, stop in the wafer in which it was produced and create a "neutral

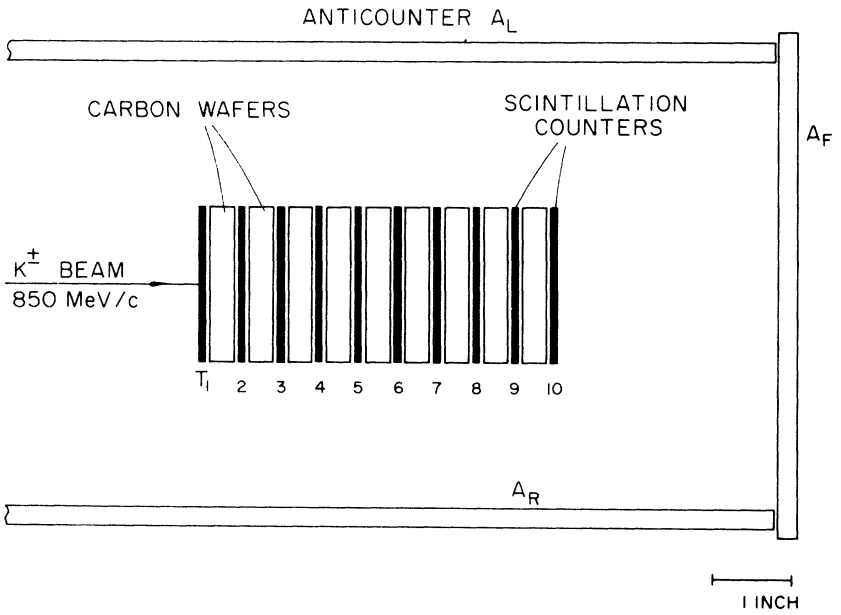

FIG. 2. Plan view of the target assembly.

TABLE I. Statistics of high-pulse-height latches.

Number of high-pulse-height latches	K^+ (percent)	K^- (percent)
0	53.2	70.0
1	30.6	20.0
2	8.6	4.7
3	2.5	0.9
4	1.0	0.6
5	0.4	0.2
Other	2.8	2.0
Discarded	0.9	1.6
Total	100.0	100.0

ending" signal just as in the K^- case. 53% of all detected K^+ events are of this kind.

In both these "neutral ending" cases the interaction is assigned the position of the center of the target wafer beyond the last set latch.

On the other hand, if the interaction occurs in a scintillator or if the recoil, cascade, or evaporation prongs escape into neighboring scintillators a "charged ending" may occur as in example 2, where two high-threshold latches are set at the end of the string.

Example 2 – a charged ending:

Low-threshold latches 1 1 1 1 1 1 1 0 0 0,
High-threshold latches 0 0 0 0 0 1 1 0 0 0.

If only one high-threshold latch is set, we assume that the charged products could have gone backwards or forwards, so the interaction is assigned the position of the scintillator itself. In all other cases, where more than one high-threshold latch is set, the charged reaction products are assumed to have gone forward. The percentages of events with various numbers of high-pulse-height latches set are given in Table I.

The category in Table I denoted with "other" consists of events where one additional high-threshold latch was set at random within a block of low-threshold latches. This latch was ignored, and the event was treated as described above. Only about 1% of the reconstructed triggers had to be discarded because of an inconsistent latch combination.

For neutral latch endings, the production point along the beam direction is thus measured to one-half the average spacing of two adjacent T counters, namely ±0.230 in. For charged latch endings, the uncertainty is twice as large. Using the weights given in Table I, we find an average uncertainty of ±0.338 in. for the K^+ data and ±0.298 in. for the K^- data. This corresponds to about $\pm 0.25 K_S$ lifetime for both charges.

The error in transverse position of the production point is caused equally by the error in beam track reconstruction (±0.030 in.) and by multiple scattering within the target (±0.030 in.). This is an order of magnitude smaller than the longitudinal uncertainty.

C. Detection and Measurement of the Decay Products

The target was surrounded by anticoincidence counters A_L, A_R, and A_F. The observed decays of the neutral kaons took place in the region between these anticoincidence counters and the three sets of wire chambers (Fig. 1). The efficiency of these anticoincidence counters (operated in a dead time-less mode) was measured to be 99.99%.

The decay region itself had different lengths in different directions and the decaying neutral kaons had varying momenta, but, roughly speaking, it extended from 4 to 13 K_S lifetimes. This region was filled with a helium bag to minimize neutron interactions that might simulate decays. We found no evidence for any background of neutron induced events.

The decay pion trajectories were determined by the three sets of wire spark chambers, one in front, one to the right, and one to the left of the beam. Each set of chambers was composed of one small (24 in.×24 in.), one medium (36 in.×36 in.), and one large (48 in.×48 in.) chamber. These chambers had their wires running horizontally and vertically. Between the small and medium chambers was an "angle" chamber with its wires making angles of ±arctan0.2 with the horizontal. This chamber served to resolve multiple-track-pairing ambiguities. Each of these chambers had a gap of $\frac{3}{8}$ in. between wire planes and consisted of 2.6×10^{-3} radiation length of material.

An event was recorded, i.e., the chambers were triggered, when a kaon decayed so as to produce two charged particles. One of these had to pass through a hodoscope of eight counters in the forward direction, R_{FRONT} in Fig. 1. The other could trigger any other counter in the hodoscope R_{FRONT} or in the seven-counter hodoscopes R_{RIGHT} or R_{LEFT}. Each counter in these hodoscopes was 8 in. wide, 48 in. high, and $\frac{1}{4}$ in. thick. If any three or more of these counters triggered, the event was rejected.

In order to reduce spurious triggers from interactions in the chamber material, a count was required in either of two W counters, $\frac{1}{16}$ in. thick and together 24 in.×24 in., placed immediately upstream of the small front chamber.

Finally, an anticoincidence counter, A_B, was placed in the beam behind the final hodoscope counters. The over-all trigger requirement was

$B_1T_1C_K\bar{C}_\pi R_F$ (any 2 from R_F or $R_{\rm SIDE}$)

$(W_1$ or $W_2)\bar{A}_F\bar{A}_L\bar{A}_R\bar{A}_B\bar{R}^3$.

This same trigger requirement was used for both polarities because the number of good events vetoed by recoil protons in K^0 production was tolerably small (35%).

Besides surveying the chamber positions, we checked the alignment of the chambers by a series of test runs using cosmic-ray tracks, antiproton annihilations in copper, and πp elastic scattering. These runs were made primarily to get the relative alignment of the front and side sets of chambers. In no case was a chamber or target position found to deviate from its surveyed position by more than 0.025 in. Appropriate corrections were made.

When the two pion tracks from a kaon decay are extrapolated toward an intersection, they have some distance of closest approach, called $d_{\rm miss}$. Figure 3 shows a distribution of this distance of closest approach for tracks extrapolated from the front and one set of side chambers (typical of neutral kaon events). An acceptable event had two tracks intersecting in the decay region with $d_{\rm miss} \leq 1.2$ cm. About 45% of the K^+ triggers and 63% of the K^- triggers satisfied this criterion. This asymmetry occurs because K^- mesons produce many Λ^0 particles as well as $\bar{K}^0$ mesons.

D. The Range Material

In order to help discriminate against decays of Λ particles, 2-in.-thick aluminum slabs (with a suitable hole for the beam) were interposed between the large spark chambers and the hodoscope counters. This aluminum stopped pions with momenta less than 135 MeV/c and protons of momenta less than 450 MeV/c and made possible a suppression of the Λ^0 contamination to $\leq 0.4\%$ of the $\bar{K}^0$ decays (see Sec. III A).

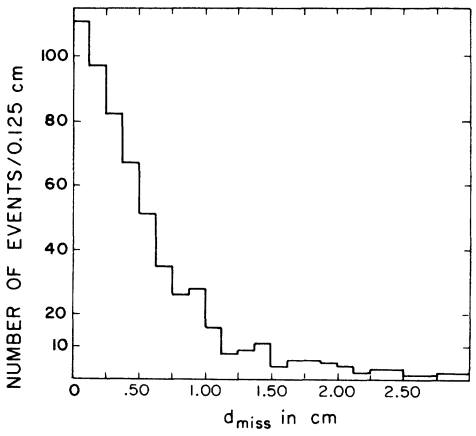

FIG. 3. $d_{\rm miss}$ distributions (distance of closest approach) for events with one track in the front quadrant and the other track in the right quadrant.

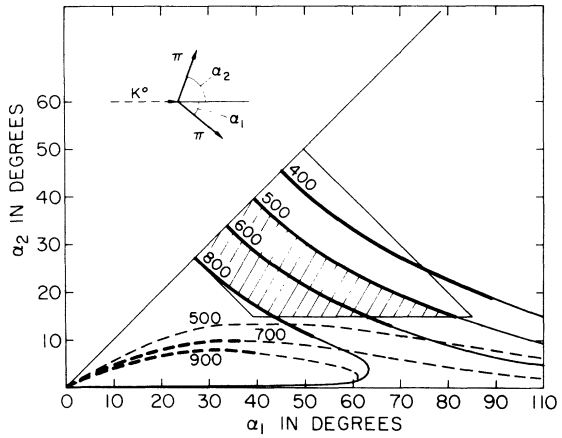

FIG. 4. Two-body decay kinematics of K^0, $\bar{K}^0$ (solid curves), and Λ^0 (dash curves). Heavy parts of the momentum contours represent events for which both decay products can penetrate through 2 in. of aluminum. The diagonal lines (corresponding to opening angles of 54 and 100 deg) and the horizontal line (representing a minimum angle of 15 deg relative to the neutral particle) are the geometrical cuts on the data. Events actually used come from the shaded region between 500 and 800 MeV/c.

E. Data Storage and On-Line Analysis

The digitized spark coordinates and the latches were read into the University of Illinois (Xerox Data Systems) Sigma 2 computer and written onto magnetic tape. The time between ZGS pulses was spent to analyze completely some 70% of the events. On-line histograms of spark distributions for each chamber as well as quadrant resolutions served to monitor the performance of the spark chambers. The experiment yielded 50 data tapes with a total of 1.1×10^6 triggers.

III. TREATMENT OF DATA

Comparison of the $\pi\pi$ decay distributions of K^0 and $\bar{K}^0$ depends on analyzing the K^+ and K^- data samples in a completely symmetric way. Potential sources of asymmetry are the Λ^0 production in K^- interactions, discussed in Sec. III A, and differences in K^0 and $\bar{K}^0$ production mechanisms, discussed in Sec. III B. In Sec. III C we discuss the $K^0, \bar{K}^0$ decay distributions with particular reference to three-body decays.

A. Λ Cuts

The production of Λ's in interactions like

$K^- + p \to \Lambda^0 + \pi^0$

and the subsequent decay $\Lambda^0 \to p\pi^-$ constitutes the principal asymmetry between K^- and K^+ data samples. This problem requires study because the over-all Λ/K detection ratio is 33 in our apparatus. Fortunately, Λ and K decays are restricted to very different kinematical regions (Fig. 4). If α_1 and α_2 are the angles between the neutral particle and its two decay products, then $\alpha_1 + \alpha_2$ is the opening angle. The $K \to \pi\pi$ decays are characterized by opening angles larger than 54 deg. Nearly all of the $\Lambda^0 \to p\pi^-$ decays with opening angles larger than 54 deg are excluded by the requirement that the decay products pass through 2 in. of aluminum range material.

Further suppression of Λ's is accomplished by placing a lower limit on the α_1 or α_2 angle between the neutral particle and one of its decay products. The proton or π^- always makes an angle less than 15 deg with the Λ direction.

The cuts are shown on Fig. 4 surrounding the accepted region for K^0 and $\bar{K}^0$ decays:

(1) opening angle between 54 and 100 deg,

(2) minimum angle $\alpha_{\min} \geq 15$ deg between the neutral decaying particle and either charged decay product,

(3) $K^0, \bar{K}^0$ momentum $500 \leq p_K \leq 800$ MeV/c.

The total Λ^0 contamination remaining in the $\bar{K}^0$ sample after making these cuts was estimated by selecting events with opening angles between 30 and 50 deg. This is the region lying below and to the left of cut (1) in Fig. 4, where the Λ^0 decays have their largest values of $\alpha_{\min}$. These events, essentially all Λ^0 decays, are plotted vs $\alpha_{\min}$ in Fig. 5(a). The small tail with $\alpha_{\min} \geq 15$ deg comprising 0.4% of the events must consist of three-body decays or poorly measured $\Lambda \to p\pi$ decays. Thus at most 0.4% of all Λ^0 decays have $\alpha_{\min} \geq 15$ deg.

Ignoring cut (2) only, one obtains a combination of $\bar{K}^0$ and Λ^0 events with opening angles between 54 deg and 100 deg [Fig. 5(b)]. The range material requirement greatly suppresses Λ^0 decays here so that the ratio of events with $\alpha_{\min} < 15$ deg to those with $\alpha_{\min} \geq 15$ deg is 0.85 (fewer Λ's than kaons). Cut (2) removes these Λ^0 decays, and the result of the preceding paragraph implies that the remaining Λ^0 contamination in the $\bar{K}^0$ decays must be less than 0.4%. One can show that this contamination does not increase as a function of "K_S" proper time.

Similar considerations apply to the Λ 3-body decays. With the requirement $\alpha_{\min} \geq 15$ deg, in the interval 4–12 K_S lifetimes, the Λ 3-body rate is less than 1% of the 3-body K decay rate.

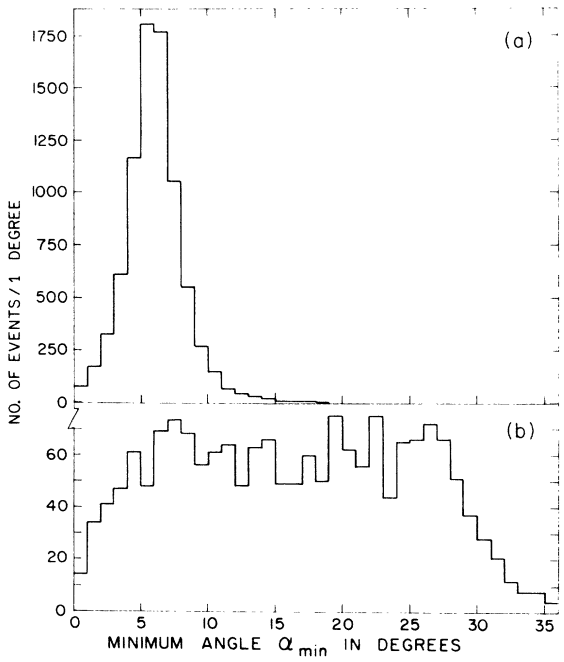

FIG. 5. Distributions of events with respect to the smaller angle $\alpha_{\min}$ (or α_1) between the neutral particle and one of its decay products: (a) for events with opening angles between 30 and 50 deg (Λ^0 decays), and (b) for events with opening angles between 54 and 100 deg and kaon momentum between 500 and 800 MeV/c.

B. Geometrical Detection Efficiency

A Monte Carlo program was written to compute the geometrical detection efficiency of our apparatus. It was tested on a selected sample of $\Lambda^0 \to p\pi^-$ events. Figure 6 shows the data points corrected for their geometrical efficiency. The straight line represents a least-squares fit to the data yielding a Λ^0 lifetime of $\tau_\Lambda = 2.52 \times 10^{-10}$ sec. The error from statistics alone would be ±1.5%; however, the uncertainty in the efficiency could be appreciably larger. The good agreement between the measured lifetime and the world average[11] of $(2.521 \pm 0.021) \times 10^{-10}$ sec lends confidence to the efficiency computation and the over-all consistency of the data.

Figure 7 shows the geometrical detection efficiency computed for K^0 or $\bar{K}^0$ decays. Since this efficiency is a function of the proper time, substantial differences in the momentum or angular distributions of K^0 and $\bar{K}^0$ mesons produced in carbon might give rise to spurious asymmetries in our data. Figure 8 shows that the momentum and angular distributions of the K^0 and $\bar{K}^0$ mesons produced in our experiment are indeed very similar to each other. The Monte Carlo calculations indicate that asymmetries greater than those allowed by Fig. 8 would make no significant difference in our results.

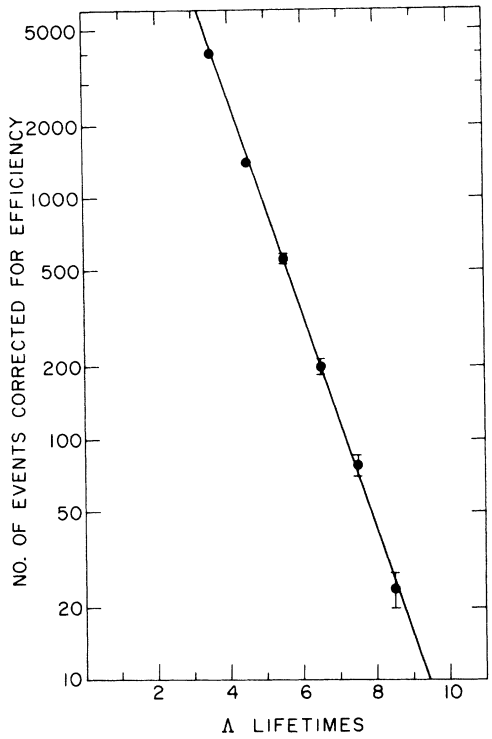

FIG. 6. Proper time distribution of Λ^0 decays. The points are the data corrected for geometrical efficiency. The straight line represents a least-squares fit to the data yielding a Λ^0 lifetime of $\tau_\Lambda = 2.52 \times 10^{-10}$ sec. The standard deviation from statistics is ±1.5%, but the uncertainty in the efficiency calculation may be appreciably larger.

C. Three-Body Decays

After the cuts to remove the Λ contamination are made, the remaining events are nearly all two- or three-body decays of K^0 and $\bar{K}^0$. The proper time for each decay was computed from the kaon flight path and the kaon momentum. The latter, being determined primarily by the opening angle between the decay pions, is known to about 1%. The principal error in the decay time is caused by our uncertainty in the production point. In the final analysis, this is a negligible error.

Figure 9 shows the proper time distributions of K^0 and $\bar{K}^0$ decays. These form the principal data of this experiment. At small decay times the decay rate (corrected for efficiency) drops exponentially with the K_S lifetime. At long times ($t > 10\,\tau_S$), the curves level off as expected for K_L decays. If these decays observed at long lifetimes were caused by some spurious effect, e.g., neutron interactions in the gas, reconstruction into decays of random background tracks, etc., we would

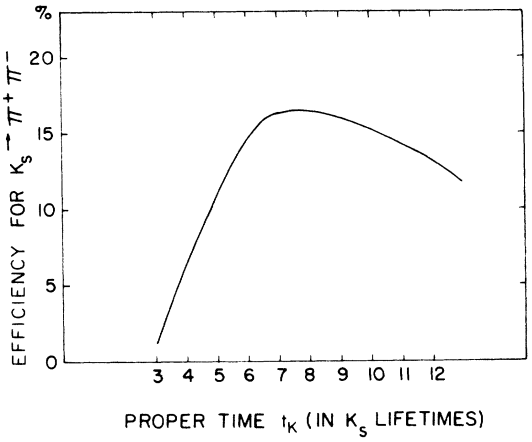

FIG. 7. Monte Carlo computation of the geometrical detection efficiency vs proper time for $K^0, \bar{K}^0$ decays. The estimated error is ±6% overall. Within the error, the efficiencies for K^0 and $\bar{K}^0$ are equal.

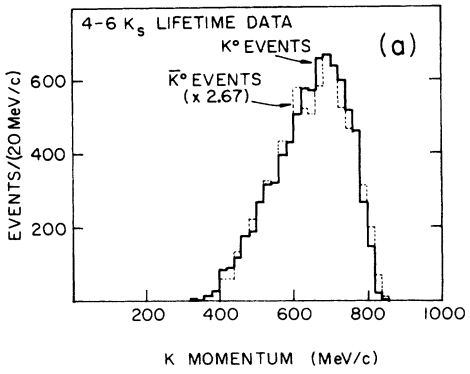

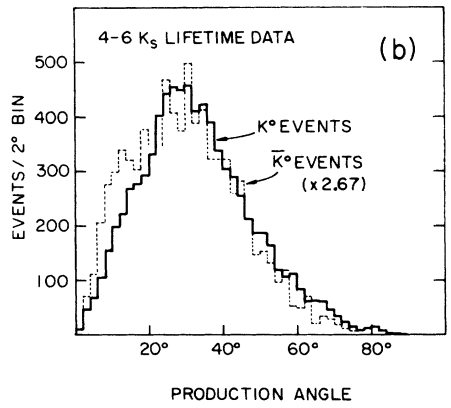

FIG. 8. Production distributions of K^0 (solid) and $\bar{K}^0$ (dotted) mesons as a function of momentum (a) and of production angle (b). Events corresponding to 4–6 K_S lifetimes are used and are normalized in this interval.

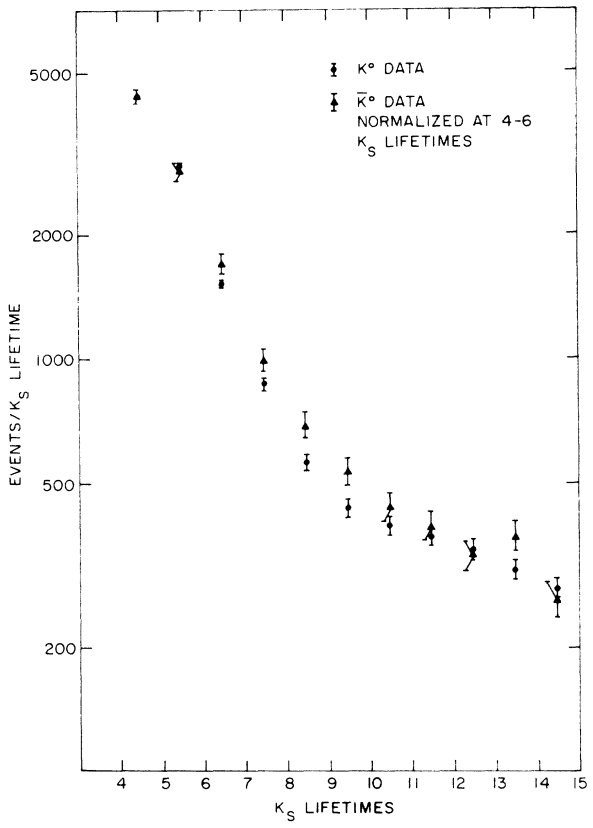

FIG. 9. Proper time distributions of K^0 and $\bar{K}^0$ decays normalized at 4 to 6 K_S lifetimes but not corrected for efficiency.

need to treat the background in a different manner for K^0 and $\bar{K}^0$ mesons and raise the possibility of introducing an asymmetry into the experiment. It is reassuring to find that this leveling off can be attributed almost completely to three-body decays of the kaon. We investigated these events in several different ways.

1. Coplanarity. Two-body decays are coplanar; three-body decays need not be. Figure 10 shows the distribution of K^0 events as a function of the cosine of the angle between the kaon direction and the normal to its decay plane ($\cos\theta_{\text{copl}}$). In the absence of any measurement errors, $\cos\theta_{\text{copl}} = 0$ for two-body decays, whereas three-body decays exhibit a broad distribution. Thus events from 3 to 4 τ_S are almost entirely two-body decays [Fig. 10(a)], whereas from 12 to 13 τ_S only three-body decays remain[12] [Fig. 10(c)].

The ratio of various types of three-body decays to two-body decays is known. A Monte Carlo program used the measured number of two-body decays at 6–7 τ_S to predict the total number of three-body decays at large decay times ($\geq 12\tau_S$). The ratio of expected three-body decays to observed events at large lifetimes was 0.99 ± 0.09. Therefore the noncoplanar background rate agrees quantitatively with that expected from three-body decays.

2. Equality of K^0 and $\bar{K}^0$ rates at large decay times. The ratio of three-body decays to two-body decays at small lifetimes should be the same for K^0 and $\bar{K}^0$. We therefore form the ratio

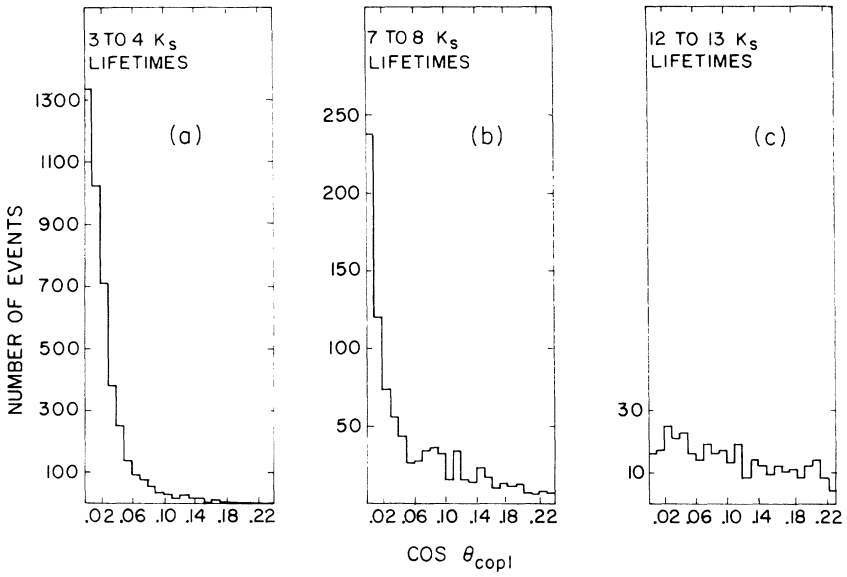

FIG. 10. Coplanarity distributions for K^0 decays at (a) 3 to 4 τ_S, (b) 7 to 8 τ_S, (c) 12 to 13 τ_S.

$$R=\left(\frac{\text{No. events } 4-6\ \tau_S}{\text{No. events}>11\ \tau_S}\right)_{K^0}\Big/\left(\frac{\text{No. events } 4-6\ \tau_S}{\text{No. events}>11\ \tau_S}\right)_{\bar{K}^0}$$

and find $R=1.04\pm0.04$. The interval 4–6 τ_S was chosen because the interference term is expected to pass through zero at the center of this interval.

3. Other checks. During the running of the experiment various other checks were made on the validity of the data. (a) Added material was placed in the decay region to see if spurious events would be found coming from it, induced perhaps by neutrons. The results showed this background to be negligible as rough estimates had predicted. (b) Pion beams, rather than kaon beams, were used with no significant number of events produced. (c) The carbon wafers were removed, and events were reduced to those expected for the remaining scintillator.

Since we find no evidence of any significant number of spurious events or spuriously reconstructed events, we conclude that within a few percent, our data consist entirely of two- and three-body decays of K^0 and $\bar{K}^0$. Figure 9 shows that the K^0 and $\bar{K}^0$ have different decay distributions. If one assumes that they can be described by the same distribution, the resulting confidence level is less than 0.01%. Such a difference is a violation of *CP* invariance in neutral K decay independent of any decay formalism. A more detailed analysis of the data is presented in Sec. IV.

IV. RESULTS

In this section we combine and summarize the results presented above by isolating the interference term in the $K^0(\bar{K}^0)\to\pi^+\pi^-$ decay distributions. Since the decay distributions shown in Fig. 9 contain contributions from both two-body and three-body K decays, the number of detected events per K_S lifetime at proper time t can be written as

$$R^{\pm}(t)=R_0^{\pm}[e^{-\gamma_S t}\pm 2|\eta|\cos(\Delta m t-\phi)e^{-(\gamma_S+\gamma_L)t/2}+|\eta|^2e^{-\gamma_L t}]+B^{\pm}(t)\ , \tag{2}$$

where $R_0^{\pm}$ are normalization constants, and $B^{\pm}(t)$ represent the background from three-body K decay. The upper sign refers to the K^0 decay distribution, the lower one to the $\bar{K}^0$ distribution. The relative normalization (i.e., the ratio R_0^+/R_0^-) represents the relative strength of the K^0 and $\bar{K}^0$ sources and can be determined from our data in two independent ways.

The first method of determining the relative normalization uses the data in the decay distributions at long proper times, i.e., the three-body K decays. In our data, the number of K^0 and $\bar{K}^0$ events with $t>12\,\tau_S$ would be equal if the strengths of the K^0 and $\bar{K}^0$ sources were equal. Conversely, the number of three-body decays with $t>12\,\tau_S$ can be used to determine the relative normalization. We find

$$\alpha\equiv\frac{R_0^+}{R_0^-}\approx\left[\frac{B^+(t)}{B^-(t)}\right]_{t>12\tau_S}=2.48\pm0.17\ . \tag{3}$$

A second and independent method for determining the relative normalization uses the number of $K^0(\bar{K}^0)\to\pi^+\pi^-$ events in the decay distributions at early proper times. From the coplanarity distribution, shown in Fig. 10, we estimate that 85% of the events in the decay distributions with proper times in the interval $6\leq t\leq 7\ \tau_S$ are $K^0(\bar{K}^0)\to\pi^+\pi^-$ decays, whereas the remaining 15% are three-body K decays. Consequently, a determination of the number of $K^0(\bar{K}^0)\to\pi^+\pi^-$ decays in this time interval is insensitive to the details of the prescription used to make a background subtraction. Using the number of $K^0(\bar{K}^0)\to\pi^+\pi^-$ decays in the interval $6\leq t\leq 7\ \tau_S$ we find

$$\alpha=\frac{R_0^+}{R_0^-}=2.64\pm0.16\ . \tag{4}$$

The agreement between these two independent determinations of the relative normalization implies that there are no large biases in the data in the decay distributions. Such agreement would, in general, not be found unless both the two-body and three-body events originated from K decay.

In terms of the relative normalization constant α, the difference between the $K^0\to\pi^+\pi^-$ and $\bar{K}^0\to\pi^+\pi^-$ decay rates is

$$\Delta R(t)=\alpha R^-(t)-R^+(t)=-4R_0^+|\eta|\cos(\Delta m t-\phi)e^{-(\gamma_S+\gamma_L)t/2}\ . \tag{5}$$

We factor out the cosine term to compare it with our data as follows:

$$D(t)\equiv\frac{\alpha N^-(t)-N^+(t)}{4R_0^+|\eta|N_0(t)}=-\cos(\Delta m t-\phi)\ , \tag{6}$$

where $N^{\pm}(t)$ are the numbers of $K^0,\bar{K}^0$ decays observed between $t-\frac{1}{2}\tau_S$ and $t+\frac{1}{2}\tau_S$, and

$$N_0(t)=\int_{t-\tau_S/2}^{t+\tau_S/2}e^{-(\gamma_S+\gamma_L)u/2}\,du\ .$$

The value $R_0^+=(4.28\pm0.21)\times10^5/\tau_S$ is obtained from the number of $K^0\to\pi^+\pi^-$ decays in the interval $6\leq t\leq 7\ \tau_S$ as described above. Other values used in Eq. (6) are

$$|\eta|=1.96\times10^{-3}\ ,$$

$$\Delta m=0.468/\tau_S\ ,$$

$$\phi = 43 \text{ deg} ,$$

$$\tau_S = \gamma_S^{-1} = 0.862\times10^{-10} \text{ sec} ,$$

$$\tau_L = \gamma_L^{-1} = 5.172\times10^{-8} \text{ sec} .$$

Figure 11 shows the comparison of our data with the cosine term according to Eq. (6). Experimental values are corrected for detection efficiencies, and noncoplanar events are excluded after making sure that the result is insensitive to the cutoff. The indicated errors include both statistical and normalization uncertainties. Within these errors, the data agree with the predicted distribution.

As emphasized in the Introduction, this experiment is probably unique in that it represents the only large sample of both K^0 and $\bar{K}^0 \to \pi^+\pi^-$ decays, taken under the same conditions with the same apparatus. This novel feature of the experiment enables us to present our data in a variety of ways. We have chosen to ask how well our data support the contention that the *CP*-violating parameters $|\eta|$ and ϕ have the same numerical value in $\bar{K}^0 \to \pi^+\pi^-$ decay as they do in $K^0 \to \pi^+\pi^-$ decay. We emphasize that this is a phenomenological interpretation of the data. Our motivation for presenting the data in this somewhat unconventional manner arises from the observation that there is essentially no experimental data in the interference region on vacuum regeneration from a pure $\bar{K}^0$ source.

Let the symbols $|\bar{\eta}|$ and $\bar{\phi}$ represent the magnitude and phase of the *CP*-violating amplitude in $\bar{K}^0 \to \pi^+\pi^-$ decay. With this notation, the theoretical side of Eq. (6) for $D(t)$ is rewritten

$$D(t) = -\frac{|\bar{\eta}|\cos(\Delta m t - \bar{\phi}) + |\eta|\cos(\Delta m t - \phi)}{2|\eta|} .$$

We have fitted our experimental data to this phenomenological model by treating $|\bar{\eta}|$ and $\bar{\phi}$ as parameters but constraining $|\eta|$, ϕ, Δm to their measured values. The resulting values

$$|\bar{\eta}| = (3.5 \pm 1.4)\times10^{-3}$$

and

$$\bar{\phi} = 66 \pm 21 \text{ deg}$$

are consistent with equality of the *CP*-violating parameters in $K^0 \to \pi^+\pi^-$ and $\bar{K}^0 \to \pi^+\pi^-$ decays.

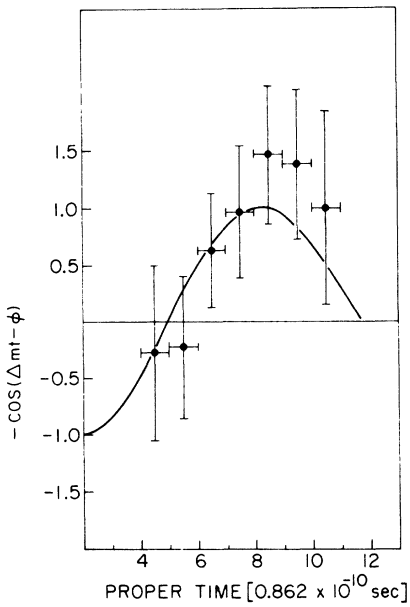

FIG. 11. The difference between $\bar{K}^0$ and K^0 decays as given by expression (6) of the text. The points are experimentally determined values of $D(t)$, and the curve is $-\cos(\Delta mt-\phi)$.

In conclusion, our results can be summarized as follows:

(1) The $K^0(\bar{K}^0) \to \pi^+\pi^-$ decay distributions provide a direct confirmation of *CP* violation independent of the conventional assumptions used in the description of the neutral kaon system.

(2) The fitted values of the parameters $|\bar{\eta}|$ and $\bar{\phi}$ are in reasonable agreement with the much more precisely determined values of $|\eta|$ and ϕ.

ACKNOWLEDGMENTS

The authors wish to thank the members of Argonne's High Energy Facilities group, particularly Dr. Irwin Spirn, for generous assistance in setting up and maintaining the beam. David Eitelbach and Robert Cullum contributed greatly to the success of the experiment by developing programs for the on-line computer analysis. We are grateful to Roger Taylor for setting up the computer facility, to Leonard Seward and Cloyd Smock for technical assistance, and to Phil Schaadt for assistance during the run.

---

*Work supported in part by the U. S. Atomic Energy Commission.

†Present address: Lawrence Livermore Laboratory, Livermore, Calif. 94550.

‡Present address: Los Alamos Scientific Laboratory, Los Alamos, N. M. 87544.

§Present address: Physics Department, Harvard University, Cambridge, Mass. 02138.

[1]J. H. Christenson, J. W. Cronin, V. L. Fitch, and R. Turlay, Phys. Rev. Letters 13, 138 (1964).

[2]J. J. Sakurai and A. Wattenberg, Phys. Rev. 161, 1449 (1967).

[3]A. Böhm, P. Darriulat, C. Grosso, V. Kaftanov, K. Kleinknecht, H. L. Lynch, C. Rubbia, H. Ticho, and K. Tittle, Nucl. Phys. B9, 606 (1969).

[4]T. D. Lee, R. Oehme, and C. N. Yang, Phys. Rev. 106, 340 (1957).

[5]P. Darriulat, J. P. Deutsch, K. Kleinknecht, C. Rubbia, and K. Tittel, Phys. Letters 29B, 132 (1969). This paper deals with the evidence one can obtain concerning particle mixtures from various thicknesses of regenerators. The arguments used depend to some extent on the hypothesis that if they exist, the other K mesons will have anomalous cross sections even though they are strongly produced.

[6]P. K. Kabir, Phys. Rev. Letters 22, 1018 (1969).

[7]D. I. Llalović, Phys. Rev. Letters 21, 1662 (1968).

[8]D. A. Jensen, S. H. Aronson, R. D. Ehrlich, D. Fryberger, C. Nissim-Sabat, and V. L. Telegdi, Phys. Rev. Letters 23, 615 (1969).

[9]The indirect evidence also depends on values of other parameters such as τ_S and η_+.

[10]D. Banner and I. Spirn, ANL Report, 1971 (unpublished).

[11]Particle Data Group, Phys. Letters 39B, 1 (1972).

[12]If an event is a three-body decay, its momentum, reconstructed on the basis of a supposed two-body decay, is approximate. Consequently its calculated decay time is only approximate. Whenever a three-body decay time is mentioned, we refer to this "fake" decay time. All three-body Monte Carlo calculations also were made on this basis. The observed rates do not, of course, include *all* three-body decays. Most of these give decay angles or reconstructed momenta eliminated by our cuts.